Electronic Supplementary Material (ESI) for Dalton Transactions.

The crystal and defect structure of polar $KBiNb_2O_7$

Subhadip Mallick, Weiguo Zhang, Maria Batuk, Alexandra S. Gibbs,
Joke Hadermann, P. Shiv Halasyamani and Michael A. Hayward*

Supporting Information

Table of Contents

1. Structural characterisation of $KBiNb_2O_7$.

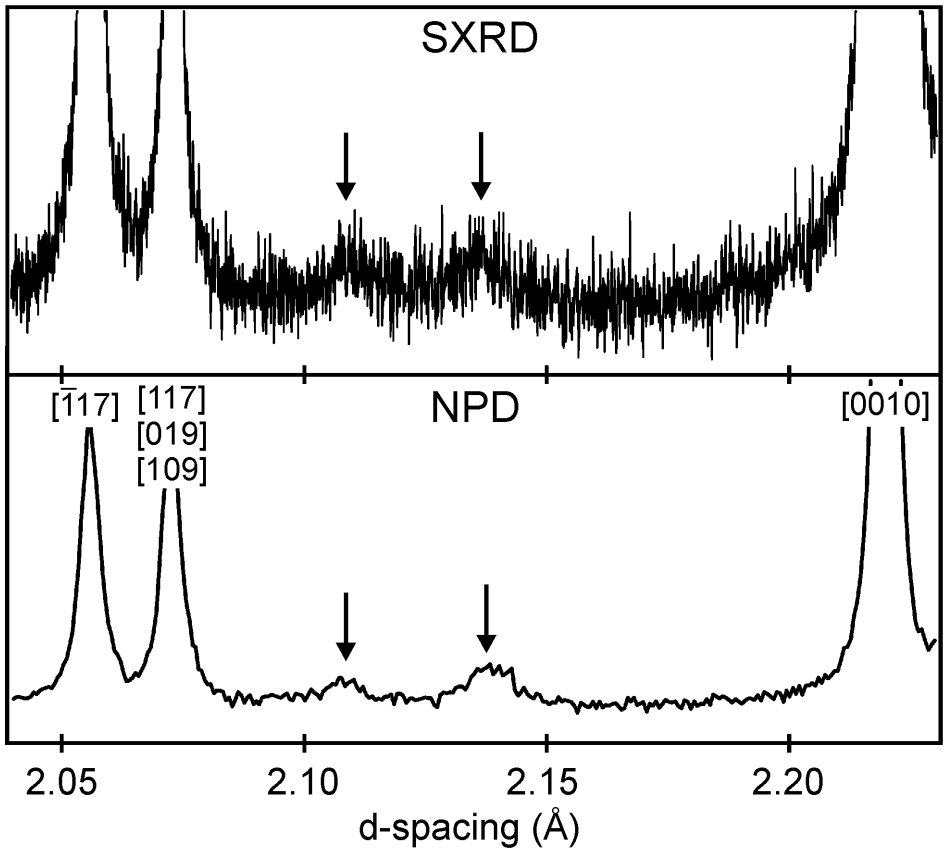

Figure S1. Selected regions of SXRD (top) and NPD (bottom) data collected from $KBiNb_2O_7$ at room temperature, indexed using the small *a* = 3.847 Å, *b* = 3.840 Å, *c* = 22.193 Å, γ = 90.80° unit cell. Arrows indicate the peaks which require the doubling of *a* lattice parameter.

Space group	no of parameters	R_p(%)	$_wR_p$ (%)
*A*11*a*	126	7.69	8.50
*A*11*m*	128	7.54	8.43
*A*112	102	8.72	10.24

Table S1. Fitting parameters from the structural refinement of different A-centred, monoclinic structural models of $KBiNb_2O_7$ against NPD data collected at room temperature.

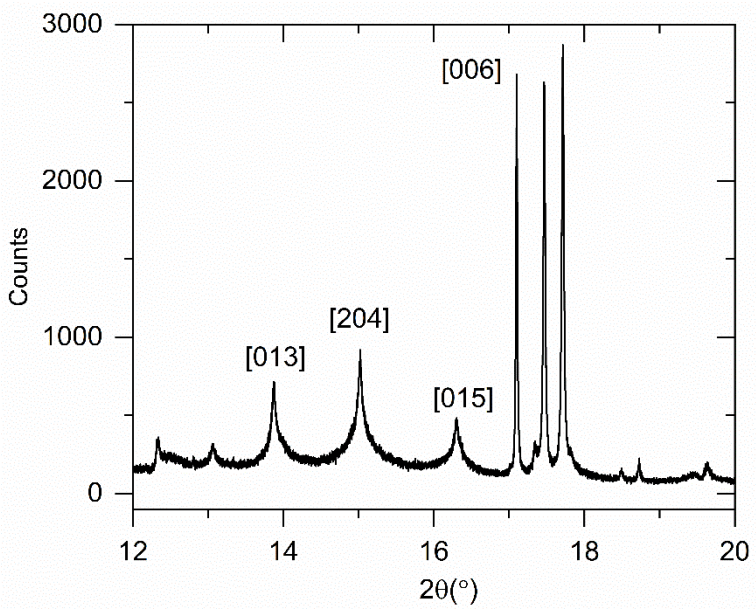

Figure S2. A section of the SXRD data collected from $KBiNb_2O_7$ which exhibits a strongly *hkl*-dependent peak width; indicative of stacking faults.

Cation	Anion	Bond length (Å)	BVS
Nb(1)	O(1)	2.329(3)	Nb+5.22
	O(3)	1.960(11)	
	0(4)	1.945(11)	
	O(5)	1.779(7)	
	O(7)	1.941(6)	
	O(7)	2.009(6)	
Nb(2)	O(2)	2.331(3)	Nb+5.12
	O(3)	1.971(11)	
	O(4)	1.973(11)	
	O(5)	1.779(7)	
	O(8)	1.954(6)	
	O(8)	2.000(6)	
Bi(1)	O(1)	2.292(20)	Bi+2.58
	O(1)	2.574(20)	
	O(2)	2.853(18)	
	O(2)	3.252(19)	
	O(3) × 2	2.463(18)	
	O(3) × 2	3.020(21)	
	O(7) × 2	2.878(12)	
	O(8) × 2	2.655(11)	
Bi(2)	O(1)	2.804(18)	Bi+2.61
	O(1)	3.296(19)	
	O(2)	2.311(20)	
	O(2)	2.540(20)	
	O(4) × 2	2.453(18)	
	O(4) × 2	3.028(20)	
	O(7) × 2	2.657(11)	
	O(8) × 2	2.866(12)	
K(1)	O(3)	3.081(24)	K+1.27
	O(3)	3.105(24)	
	O(5)	2.763(26)	
	O(5)	2.941(26)	
	O(5)	3.379(19)	
	O(6)	2.487(26)	
	O(6)	2.755(26)	
	O(6)	3.186(18)	
	O(7)	3.248(19)	
	O(8)	2.890(18)	
K(2)	O(4)	2.936(20)	K+1.30
	O(4)	3.279(22)	
	O(5)	2.467(24)	
	O(5)	2.746(25)	
	O(5)	3.172(17)	
	O(6)	2.769(25)	
	O(6)	2.946(24)	
	O(6)	3.378(18)	
	O(7)	2.883(17)	
	O(8)	3.262(19)	

Table S2. Selected bond lengths from the refined structure of $KBiNb_2O_7$.

2. Microstructural characterisation of $KBiNb_2O_7$

In order to account for the strongly *hkl*-dependent peak widths observed in the diffraction patterns collected from $KBiNb_2O_7$ and to quantify the frequency of the 'axis-switch' stacking faults, we have performed a series of Rietveld refinements that include a stacking fault model as implemented in the Topas (V6) software.

A model describing a $K_2BiNb_2O_7$ block (labelled layer A) was constructed based the atomic coordinates of the *A*11*m* model obtained from refinement against neutron diffraction data (Table 1). To facilitate the calculation, the area of the *ab*-plane of the model layer was half that of the refined *A*11*m* model, and described by lattice parameters *a*' = *a*/2, *b*' = *b*, with the alternating displacement of the Bi cations parallel to the *y*-axis (which leads to the original doubling the *a* lattice parameter) neglected in the model. Thus, the model block contains 1 bismuth, 2 niobium, 2 potassium and 7 oxygen atom sites, with the locations of the atoms described using the *P*1 space group (i.e. no symmetry). A second model $K_2BiNb_2O_7$ block (labelled layer B) was constructed by taking the model of layer A and switching the *x*- and *y*-coordinates (i.e. rotating the model by 90° around the *z*-axis).

Supercells were then constructed by stacking the model layers into large arrays. As shown in Figure S3, if layer A is stacked on itself repeatedly, such that there is a (0, ½, *c*/2) shift in the origin of the blocks between adjacent layers, then a 'perfect' unfaulted structure for $KBiNb_2O_7$ is described. Likewise, if layer B is stacked on itself repeatedly, such that there is a (½, 0, *c*/2) shift in the origin of the blocks between adjacent layers, then a 'perfect' unfaulted structure for $KBiNb_2O_7$ is described, with the *x* and *y*-axes exchanged compared to the all-layer-A stack. However, if an A layer is followed by a B layer (Figure S3) such that there is a (0, ½, *c*/2) shift in the origin of the blocks between adjacent layers, or a B layer is followed by an A layer with a (½, 0, *c*/2) shift in the origin of the blocks between adjacent layers then the *x* and *y*-axes of the stack with be switched. Thus by intermixing blocks of layer A and layer B, arrays containing 'axis-switch' faults can be constructed.

Stacking faults were introduced into models using the parameter "*P*" which takes values between 0 and 1. The value of *P* describes the probability that an A layer will be followed by another A layer stacked in a (0, ½, *c*/2) manner, and 1-*P* describes the probability that an A layer will be followed by a B layer stacked in a (0, ½, *c*/2) manner. Similarly *P* also describes the probability that an B layer will be followed by another B layer stacked in a (½, 0, *c*/2) manner, and 1-*P* describes the probability that an B layer will be followed by a A layer stacked in a (0, ½, *c*/2) manner. Thus, it can be seen that concentration of axis-switch faults is equant to 1-*P*, a value which we more clearly described as *FF*, the fault frequency.

Stacking fault models with supercells of finite size were constructed by stacking N_v = 1000 $KBiNb_2O_7$ blocks. To more accurately represent the probabilistic nature of stacking faults, an average intensity from N_{str} = 100 crystals was calculated. The peak shape parameters for refinement were fixed after the first refinement with P = 1. A series of models with different values of P were refined against the SXRD data, whilst keeping the atomic coordinates of the model static, to find the value of FF which best fitted the data. The introduction of this fault description led to a great improvement in the fit to the data as shown in Figure 5. As shown in Figure 6, the best fit to the SXRD data was obtained with a value of FF = 0.09, which corresponds to a 9% chance of a stacking fault occurring between any particular pair of perovskite double sheets. This faulting probability appears to be in line with the number of faults observed in the HAADF-STEM images.

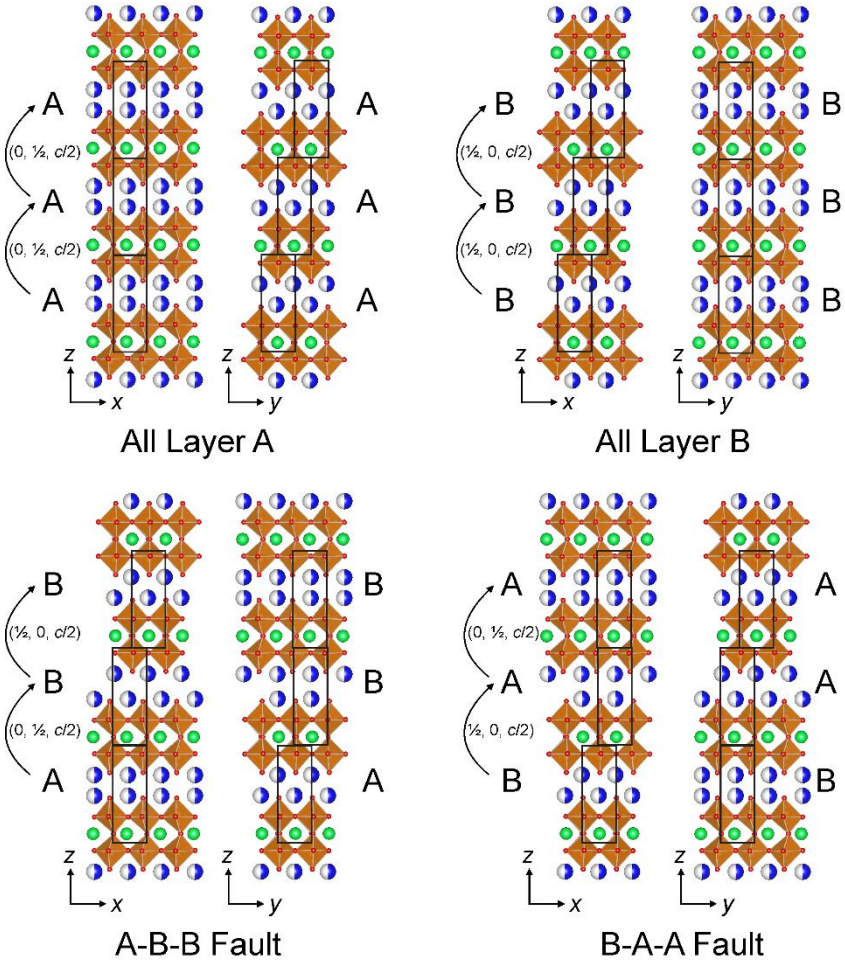

Figure S3. Schematic diagram showing the stacking of A-layers and B-layers to yield 'perfect', unfaulted structures, and the combination of A-layers and B-layers to produce stacks with 'axis-switch' faults. Black rectangles indicate the boundaries of a single block.